Structural Stability and Adatom Diffusion at Steps on Hydrogenated Si(100) Surfaces

Sukmin Jeong and Atsushi Oshiyama
Institute of Physics, University of Tsukuba, Tennodai, Tsukuba 305, Japan
(Received 25 June 1998)

We present first-principles total-energy calculations which reveal microscopic structures of the steps and mechanisms of the adatom diffusion on hydrogenated Si(100) surfaces. Energetics among several types of the steps depends on the hydrogen chemical potential μ_{H}, and the nonrebonded structure is more stable than the rebonded one for a wide range of μ_{H}. Calculations of the diffusion pathways and activation barriers for the adatom show that the Schwoebel barrier is absent near the single-layer steps. It is also found that the nonrebonded S_B step is a deep sink for the adatom in epitaxial growth. [S0031-9007(98)07908-3]

PACS numbers: 68.35.Bs, 68.35.Fx, 68.55.–a, 81.10.Aj

Steps on surfaces play a crucial role in the epitaxial growth of semiconductors [1]. In the step flow regime at high temperatures, adatoms which have been adsorbed on terraces diffuse to step edges and then are incorporated into the crystal. At lower temperatures, two-dimensional islands, where boundaries are regarded as short step edges, grow on the terraces, gathering adatoms in the vicinity. Adatom diffusion and incorporation near the step edges are thus fundamental atomic processes in the growth phenomena. In this Letter, we report first-principles total-energy calculations which reveal microscopic structures of the steps, and mechanisms of the adatom diffusion and incorporation onto hydrogenated Si(100) surfaces.

The hydrogenated Si(100) surface has been extensively studied for its importance in both science and technology [2–12]. In homoepitaxial and heteroepitaxial growth using chemical vapor deposition or gas-source molecular beam epitaxy (MBE), the growth front is terminated by H [2–6]. In solid source MBE, H is introduced intentionally to assist in epitaxial growth [7–10]. Morphology of overlayers indeed depends on H coverage [3,6,10], and even the growth mode is modified using H as a surfactant in the heteroepitaxy [7,8].

Each pair of top-layer Si atoms on the (100) surface forms a dimer, and the dimer rows are aligned along the $\langle 011 \rangle$ direction. H atoms introduced on the surface usually terminate the remaining dangling bonds leading to the 2×1 phase [13]. The dimer rows cause two distinct types of atomic steps: one where the step edge is parallel to the dimer-row direction on an upper terrace and the other where it is normal, labeled by the subscripts A and B, respectively [14]. Recent first-principles calculations have revealed that a Si adatom on a terrace of the hydrogenated surface is adsorbed substitutionally and then diffuses on the terrace via a complex mechanism where the H capture and release are essential atomic processes [11,12]. Little is known about the steps, however: Local structures and energetics of the steps and, moreover, mechanisms of the adatom diffusion near the steps and its sticking to the step edges need to be clarified.

We here report total-energy calculations within the local density approximation (LDA) for structures of single- (S) and double- (D) layer steps on the H-terminated 2×1 Si(100) surface. We find that the energetics among several types of the steps is sensitive to the H chemical potential. This leads to a possible controllability of the step morphology by changing H atmosphere. Calculated scanning tunneling microscope (STM) images facilitate microscopic identifications of the steps through comparison with experiments. We have also calculated diffusion pathways and activation energies for a Si adatom near the step edges. It is found that the H capture and release are crucial processes and that an additional activation barrier near the step edges (the Schwoebel effect [15]) is *absent* in contrast to the prevailing picture. It is also found that the S_B step is a *deep* sink for the adatom. Its implication for the morphology of overlayers is also discussed.

All calculations have been performed by use of norm-conserving pseudopotentials [16], the LDA for the exchange-correlation energy [17], and the conjugate-gradient minimization technique [18]. The surface is simulated by a repeating slab model in which five Si layers and an 8.4 Å vacuum layer are included. The bottom of the slab has a bulklike structure with each Si atom saturated by two H atoms. To simulate steps, we use the periodic step arrays on the (100) surfaces with $2 \times n$ periodicities ($n = 6$, 8, and 10) and the $(15, 1, 1)$ vicinal surfaces. The 8-Ry cutoff energy in the plane wave basis and the three k points in surface Brillouin zone (SBZ) are used [11]. It is found that the energy differences between several key geometries converge well at the 8-Ry cutoff, although a larger cutoff energy is necessary for the absolute total-energy convergence: For the total-energy difference between the stable and the saddle-point geometries on the H/Si(100)-(2×1) [11], the 8-Ry cutoff gives the converged value which is 5% (0.04 eV) smaller than the completely converged value obtained by the 30-Ry cutoff. The cutoff-energy convergence is also examined by performing the calculations for silane SiH_4. The Si-H bond length, the stretching vibrational frequency, and

 0031-9007/98/81(24)/5366(4)$15.00

the bending vibrational frequency obtained by the 8-Ry cutoff agree with the well converged values obtained by the 30-Ry cutoff with the differences of 1.2%, 3.0%, and 4.0%, respectively. Geometries are optimized for all atoms except for the bottommost Si and H atoms until the remaining force on each atom is less than 0.005 Ry/Å.

The diffusion pathways and activation energies for the adatom are calculated by the constrained optimization in a $(N-1)$-dimensional space, where N is the degree of freedom in the unit cell. We first perform an extensive search of the (meta)stable structures for the adatom. Then, for a diffusion process between the two metastable structures, we define a plane [i.e., a $(N-1)$-dimensional hyperspace] perpendicular to the line which connects the two metastable structures (i.e., N-dimensional vectors). Geometry optimization is then performed within the $(N-1)$-dimensional hyperspace. We repeat the optimization for several geometries which are initially located at different positions on the line. The 2×6 unit cell and two k points in SBZ are used for this purpose. Use of the larger unit cells with the 2×10 and 4×6 periodicities changes the activation energies by less than 0.06 eV.

Figure 1 shows calculated formation energies λ per surface lattice constant ($a = 3.84$ Å) of S_A, S_B, D_A, and D_B steps as a function of the H chemical potential μ_{H}. The formation energies of S_A, S_B, and D_B steps are calculated using the periodic step arrays with the $2 \times n$ lateral periodicity (superscripts in Fig. 1): The convergence with respect to n is assured within 50 meV/a [19]. On the other hand, $\lambda(D_A) - [\lambda(S_A) + \lambda(S_B)]$ is calculated using the $(15, 1, 1)$ vicinal surface. The local structures of the B-type steps are in sharp contrast with those on the clean surface: Rearrangement of a bond network at the step edge (rebonding) that is a principal atomic relaxation on the clean surface is found to be energetically unfavorable on the hydrogenated surface. This is a consequence of the existence of H atoms which terminate dangling bonds at the step edge. This small but important difference in the local structure manifests itself in the STM images. Figures 2(a) and 2(b) show the calculated STM images of the rebonded D_B step on the clean surface and the nonrebonded D_B step on the hydrogenated surface. The difference between the two structures is clearly seen in the images. The existence of H atoms also affects the local structures of other types of the steps: e.g., the π-bonding relaxation in the nonrebonded D_B step on the clean surface [20,21] is missing on the hydrogenated surface. On the hydrogenated surface [22], the rebonded and nonrebonded structures [Figs. 2(b) and 2(c)] are easily distinguished from the STM images: In the nonrebonded D_B step, medium-bright parts, corresponding to the H atoms bonded to the edge Si atoms, are separated by $\sim 0.8a$ from the neighbor dimers of the upper terrace, while in the rebonded D_B step, they are separated by $\sim 1.5a$. This difference is also found in the images of the single-layer steps.

In the region of the H chemical potential where the 2×1 phase is stable, formation energies λ of S_A, S_B, and D_B steps are relatively low (Fig. 1). From the calculations of the vicinal surfaces, the energy difference $\lambda(D_B) - [\lambda(S_A) + \lambda(S_B)]$ is quite small, which implies that both the D_B step and the S_A plus S_B steps are equally observable in experiments. At high temperatures, Si adatoms diffuse

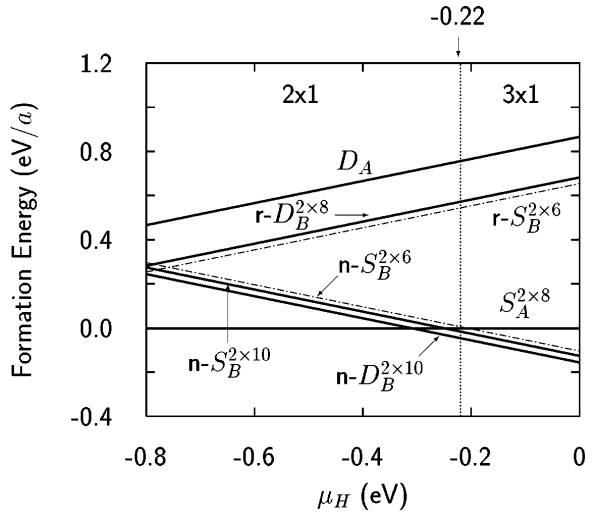

FIG. 1. Formation energies per surface lattice constant ($a = 3.84$ Å) of single-layer and double-layer steps (relative to the flat surface) as a function of hydrogen chemical potential μ_{H}. The letters "n" and "r" indicate "nonrebonded" and "rebonded," respectively. The reference of μ_{H} is the value at which SiH_4 can be formed from a reservoir of H and bulk Si with no energy cost (Ref. [13]). In the region of $\mu_{\mathrm{H}} > -0.22$ eV (vertical line), the step formation energies may be modified since the structure on the terrace changes to the 3×1 phase.

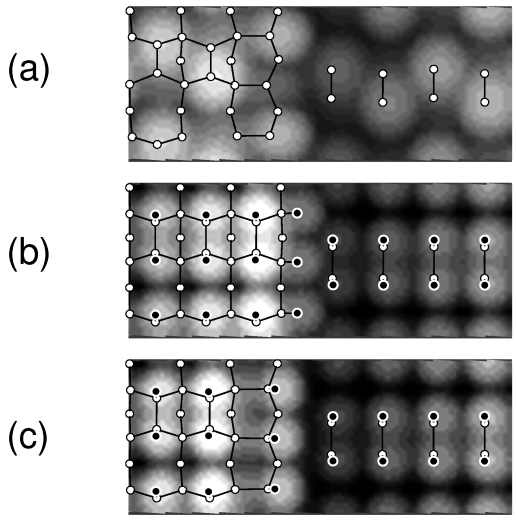

FIG. 2. Simulated STM images of (a) the rebonded D_B step on the clean surface and (b) the nonrebonded and (c) rebonded D_B steps on the hydrogenated surface (the upper terrace on the left). The bias voltages are approximately -1.6 eV with respect to the highest occupied states. Black and open circles denote H atoms and Si atoms, respectively. Bright parts, which mean higher positions of iso-electron-density surfaces, correspond to the H atoms on the hydrogenated surface, while to the up atoms of Si dimers on the clean surface (Ref. [22]).

relatively fast, tending to form their equilibrium island shapes. Anisotropic islands that are observed on the clean surface are indeed interpreted in terms of the anisotropy in $\lambda(S)$ since the boundaries of the islands are regarded as step edges [23]. However, the step formation energies are sensitive to μ_{H} on the hydrogenated surface. Calculated results thus predict that equilibrium shapes of the steps and epitaxial islands on the hydrogenated surface are controlled by changing μ_{H}, i.e., the H pressure along with temperature.

Figure 3 shows calculated diffusion pathways and activation energies for the Si adatom near the nonrebonded S_B and the S_A steps. We present one of the several pathways along which activation energies are found to be comparable. Near the nonrebonded S_B step edge, a lot of metastable sites which are not seen on the flat surface are found. An adatom from the channel between dimer rows on the upper terrace reaches a local minimum at A_1, which is essentially the same as the global minimum of the flat terrace (A_0) [11,24]. The adatom then crosses the step edge following a pathway A_1PCDM (or A_1PBDM) and finally reaches the minimum site M which is larger than A_0 in binding energy by 1.6 eV. As addressed in the previous calculations [11], the H release and capture are the crucial processes in the adatom diffusion (Fig. 4): The adatom captures a H atom ($A_1 \rightarrow P$), then releases one H atom to an upper-terrace dimer ($P \rightarrow C$), and again captures another H atom ($C \rightarrow D \rightarrow M$). The activation energy for the pathway is 0.8 eV by the $P \rightarrow C$ step. The adatom from the dimer rows of the upper terrace follows a pathway E_1PCDM. The energy barrier is again 0.8 eV with $P \rightarrow C$ as the rate-determining process. The energy barrier from the upper terrace to the lower terrace is comparable to the diffusion barrier along the dimer rows on the flat terrace ($Q_{\parallel} = 0.7$ eV [11]). Thus, there is no additional energy barrier (Schwoebel barrier [15]) in the vicinity of the step edge. On the other hand, the adatom from the lower terrace (from E_2) can reach M with a barrier of 0.4 eV. Once an adatom is captured at M, it hardly escapes from the site since the barriers toward the upper and lower terraces are as high as 1.8 and 2.0 eV, respectively. Therefore, the nonrebonded S_B step plays as a deep sink for the adatom. The stability of M comes from the formation of the adatom-dihydride in which all surface dangling bonds are terminated (Fig. 4).

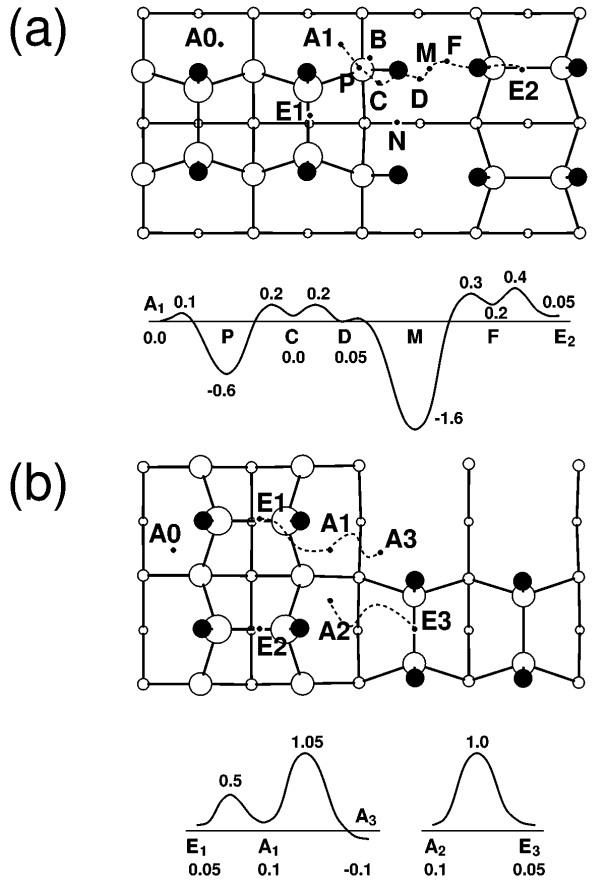

FIG. 3. Calculated diffusion pathways and activation energies for the adatom near (a) the nonrebonded S_B and (b) the S_A steps (the upper terrace on the left). Black and open circles denote H atoms and Si atoms, respectively. Small dots represent metastable sites. The structures shown in (a) and (b) are the corresponding equilibrium ones without an adatom. Values shown in the lower panels of (a) and (b) are the energies of the metastable or transition states with respect to the global minimum on the flat terrace.

The adatom reaction and diffusion near the S_A step show sharp differences from those near the nonrebonded S_B step [Fig. 3(b)]. We have found three binding sites, A_1, A_2 and A_3 near the S_A step. The binding energy of A_3 is only 0.1 eV larger than that of A_0. An adatom from the upper terrace migrates to the lower terrace along $A_1 \rightarrow A_3$ or $A_2 \rightarrow E_3$. The energy barriers for the two pathways are 0.9 and 0.95 eV, respectively, which are comparable to that for the adatom diffusion perpendicular to the dimer rows on the terrace ($Q_{\perp} = 1.0$ eV [11]). Thus, the Schwoebel barrier is again absent. Since there is no deep binding site near the step edge, the S_A step is a shallow sink for the adatom.

The absence of the Schwoebel barrier near the single-layer steps is distinct from the D_B step on the clean surface, where an adatom undergoes a large barrier for the diffusion [20]. The barrier causes a step bunching, leading to the formation of {311} facets. Such a step bunching, however, is not likely at the single-layer steps on the hydrogenated Si(100) surface.

The present finding that the S_B step is a deep sink for the adatom gives a unified explanation of several observations in epitaxial experiments. First, a denuded zone, where the island density is much reduced compared to other places, appears near the upper terrace of the S_B step during the growth [3]. Because of its anisotropic diffusion [11,12], the adatom from the upper terrace gets easier access to M than from the lower terrace near the S_B step edge. This leads to a less island density on the upper terrace. Second, antiphase boundaries that are generated when two epitaxial islands meet each other out of phase

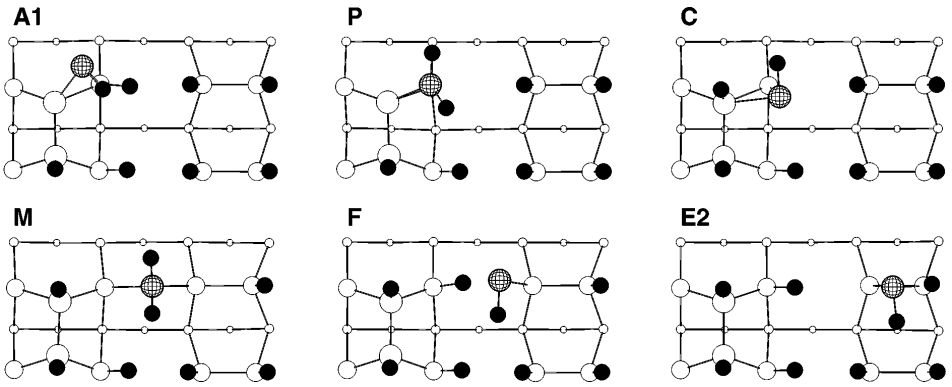

FIG. 4. Stable and metastable geometries around the nonrebonded S_B step edge. Meshed, black, and open circles denote Si adatoms, H atoms, and Si atoms, respectively. Labels correspond to the sites shown in Fig. 3(a).

(dimer rows of one island to troughs of the other and vice versa) are frequently observed in the growth using hydrogen [4,6]. The *B*-type antiphase boundaries, which are perpendicular to the dimer rows of the islands and thus structurally similar to the S_B step, are effective nucleation sites [4,6]. We argue that this phenomenon is due to the preferential adatom adsorption at the S_B steps. Finally, it was observed that hydrogen works as a surfactant in Ge/Si heteroepitaxy, suppressing the three-dimensional growth of the Ge overlayer [7,8]. Formation of the three-dimensional structures involves adatom aggregation onto islands via surface diffusion, which makes it necessary for adatoms to climb the step boundaries of the islands. On the clean Si(100) surface, the activation energies for Si adatom climbing are 0.85 and 1.4 eV near the S_A and S_B steps, respectively [25]. On the hydrogenated Si(100) surface, however, the adatom climbing is effectively prevented by larger energy barriers of 1.0 and 1.8 eV (Fig. 3). Since the present results of Si adsorption could be relevant to Ge adsorption, it is expected that the H atom works as a surfactant suppressing island formation.

This work was supported in part by the Japan Society for the Promotion of Science under Contract No. RFTF96P00203.

[1] W. K. Burton, N. Cabrera, and F. C. Frank, Philos. Trans. R. Soc. London A **243**, 299 (1951).
[2] J. J. Boland, Adv. Phys. **42**, 129 (1993), and references therein.
[3] D.-S. Lin *et al.*, Phys. Rev. B **45**, 3494 (1992).
[4] M. J. Bronikowski, Y. Wang, and R. J. Hamers, Phys. Rev. B **48**, 12 361 (1993).
[5] Y. Wang, M. J. Bronikowski, and R. J. Hamers, Surf. Sci. **311**, 64 (1994).
[6] M. Fehrenbacher *et al.*, J. Vac. Sci. Technol A **14**, 1499 (1996).
[7] A. Sakai and T. Tatsumi, Appl. Phys. Lett. **64**, 52 (1994).
[8] S.-J. Kahng *et al.*, Phys. Rev. Lett. **80**, 4931 (1998).
[9] M. Copel and R. M. Tromp, Phys. Rev. Lett. **72**, 1236 (1994).
[10] J. E. Vasek *et al.*, Phys. Rev. B **51**, 17 207 (1995).
[11] S. Jeong and A. Oshiyama, Phys. Rev. Lett. **79**, 4425 (1997), and unpublished results.
[12] J. Nara, T. Sasaki, and T. Ohno, Phys. Rev. Lett. **79**, 4421 (1997).
[13] The 3×1 and 1×1 phases appear with increasing H dose or hydrogen chemical potential. For details, see, e.g., J. E. Northrup, Phys. Rev. B **44**, 1419 (1991).
[14] D. J. Chadi, Phys. Rev. Lett. **59**, 1691 (1987).
[15] R. L. Schwoebel and E. J. Shipsey, J. Appl. Phys. **37**, 3682 (1966).
[16] N. Troullier and J. L. Martins, Phys. Rev. B **43**, 1993 (1991).
[17] D. M. Ceperley and B. J. Alder, Phys. Rev. Lett. **45**, 566 (1980).
[18] O. Sugino and A. Oshiyama, Phys. Rev. Lett. **68**, 1858 (1992); M. Saito, O. Sugino, and A. Oshiyama, Phys. Rev. B **46**, 2606 (1992); B. D. Yu and A. Oshiyama, Phys. Rev. Lett. **71**, 585 (1993).
[19] Step formation energy depends on the terrace width [O. L. Alerhand *et al.*, Phys. Rev. Lett. **61**, 1973 (1988); T. W. Poon *et al.*, *ibid.* **65**, 2161 (1990)]. The energy change with increasing terrace width, however, is quite small compared to that with μ_{H} variation (see $S_B^{2\times6}$ and $S_B^{2\times10}$ in Fig. 1).
[20] A. Oshiyama, Phys. Rev. Lett. **74**, 130 (1995).
[21] E. Kim, C. W. Oh, and Y. H. Lee, Phys. Rev. Lett. **79**, 4621 (1997).
[22] Of note is a weak splitting in the image of a dimer on the hydrogenated surface. (It is true of the unoccupied-state images). This feature agrees with a recent experiment (Ref. [5]), but not with earlier studies (Refs. [2] and [3]). The splitting is not observed for the occupied-state images of the clean surface. It is thus possible to discriminate between hydrogenated and clean dimers by observing the occupied-state images.
[23] Y.-W. Mo *et al.*, Phys. Rev. Lett. **63**, 2393 (1989).
[24] Here, the global minimum means the structure which can be reached from a Si vapor phase without any activation energy (Ref. [11]).
[25] Q.-M. Zhang *et al.*, Phys. Rev. Lett. **75**, 101 (1995).